Available online at www.sciencedirect.com
ScienceDirect
Polymer 48 (2007) 4907–4920
polymer
www.elsevier.com/locate/polymer

Feature Article

Multiwall carbon nanotube elastomeric composites: A review

Liliane Bokobza

Laboratoire PPMD, E.S.P.C.I., 10 rue Vauquelin, 75231 Paris Cedex, France

Received 17 February 2007; received in revised form 13 June 2007; accepted 16 June 2007
Available online 27 June 2007

Abstract

Nanostructured materials gained great importance in the past decade on account of their wide range of potential applications in many areas. A large interest is devoted to carbon nanotubes that exhibit exceptional electrical and mechanical properties and can therefore be used for the development of a new generation of composite materials. Nevertheless, poor dispersion and poor interfacial bonding limit the full utilization of carbon nanotubes for reinforcing polymeric media.

In this paper, recent advances on carbon nanotubes and their composites will be presented through results of the author's research, essentially based on filled elastomeric networks. The intrinsic potential of carbon nanotubes as reinforcing filler in elastomeric materials will be demonstrated. It will be shown that, despite a poor dispersion, small filler loadings improve substantially the mechanical and electrical behaviors of the soft matrix. With the addition of 1 phr of multiwall carbon nanotubes in a styrene–butadiene copolymer, a 45% increase in modulus and a 70% increase in the tensile length are achieved. Straining effects investigated by atomic force microscopy and infrared and Raman spectroscopies, provide interesting results for the understanding of the mechanical behavior of these nanotube-based composites. All the experimental data lead to the belief that the orientation of the nanotubes plays a major role in the mechanical reinforcement. The strong restriction in equilibrium swelling in toluene with the MWNT content is not ascribed to filler–matrix interfacial interactions but to the occlusion of rubber into the aggregates. On the other hand, carbon nanotubes impart conductivity to the insulator matrix. Between 2 and 4 phr, the conductivity increases by five orders of magnitude reflecting the formation of a percolating network. Changes in resistivity under uniaxial extension completed by AFM observations of stretched composites bring new insights into the properties of these composites by highlighting the contribution of orientational effects.

Keywords: Carbon nanotubes; Elastomers; Reinforcement

1. Introduction

Elastomers are usually reinforced with mineral fillers in order to get substantial improvements in strength and stiffness. The extent of property improvement depends on several parameters including the size of the particles, their aspect ratio, their degree of dispersion and orientation in the matrix and the degree of adhesion with the polymer chains [1].

The last few years have seen the extensive use of nanoparticles because of the small size of the filler and the corresponding increase in the surface area allowing to achieve the required mechanical properties at low filler loadings.

In order to create new material systems with superior properties, various nanoparticle morphologies have been used as reinforcing fillers in elastomeric matrices. These nanometer-scale reinforcing particles include spherical particles such as silica or titania [2–5], platelets such as layered silicates [6–12], carbon [13] or clay fibers [14] and multiwall or single-wall carbon nanotubes [15–17].

Sol–gel technique generating nano-sized silica or titania particles within a host matrix has proved to be an excellent approach for the synthesis of hybrid systems where the organic and inorganic components are intimately mixed into a new material exhibiting greatly improved mechanical properties.

Layered silicates have generated significant interest because they can give rise to exfoliated systems in which the individual silicate nanolayers are homogeneously and uniformly dispersed throughout the polymer matrix. The exfoliated

E-mail address: Liliane.Bokobza@espci.fr

0032-3861
doi:10.1016/j.polymer.2007.06.046

nanocomposites exhibit significantly enhanced mechanical and physical properties when compared to unfilled polymers or conventional composites.

Since their discovery in 1991 [18], carbon nanotubes (CNTs) have attracted enormous attention for their fundamental behavior and for their use in a wide variety of applications in nanoelectronic devices [19–21], probe tips for scanning probe microscopes [22–26] or in the automotive and aerospace industries for the dissipation of electrostatic charges [27,28]. Owing to their structural characteristics and their electrical and mechanical properties, one of the most important opportunities in the future is the emergence of a new generation of composite materials since relatively low carbon nanotube loading (<10 wt.%) within polymeric matrices, are required for various applications [29,30].

2. Characteristics, synthesis methods and processing of carbon nanotubes for composite materials

Carbon nanotubes can be visualized as graphene layers rolled into cylinders consisting of a planar hexagonal arrangement of carbon–carbon bonds. Their outstanding properties are a consequence of this unique bonding arrangement combined with topological defects required for rolling up the sheets of graphite into cylinders. During growth, depending on the synthesis methods, they can assemble either as concentric tubes (multiwall nanotubes, MWNTs) or as individual cylinders (single-wall nanotubes, SWNTs). Their diameters range from about a nanometer to tens of nanometers with lengths ranging from several micrometers to millimeters or even centimeters.

Carbon nanotubes can be synthesized by different techniques including arc-discharge [31,32], laser ablation [33–36] and various catalytic chemical vapor deposition (CCVD) [37–40].

In the arc-discharge technique, an electric arc is generated between two graphite electrodes under a helium or argon atmosphere, which causes the graphite to vaporize and condense on the cathode. The deposit contains the nanotubes and also fullerenes, amorphous carbon materials and catalyst particles. This technique requires further purification to separate the CNTs from the by-products present in the crude material. The electrodes of graphite are doped with catalytic metal atoms (Ni, Co) for the production of SWNTs. A high-temperature pulsed arc-discharge technique has been developed for the synthesis of single- and double-wall (DWNTs) carbon nanotubes with narrower tube diameters than those obtained with the steady arc method [41,42].

In laser ablation, a laser ablates a graphite target in flowing argon at temperatures near 1200 °C. The graphite target contains a small amount of a metal catalyst such as nickel, cobalt, iron, platinum, yttrium. It has been shown that bimetallic catalysts are more productive than single metals. Various configurations of laser ablation experiments were developed for the production of single-wall carbon nanotubes. They range from a single or a dual pulsed laser to a continuous laser. The yield, mean diameter and diameter distribution can be varied by varying the growth temperature, gas, pressure, catalyst composition, laser pulse, etc.

Small amounts of CNTs can be formed by arc-discharge and laser vaporization which is really a limitation to scale up production to the industrial level. Larger quantities of nanotubes can be obtained by the pyrolysis of a carbon source such as carbon monoxide, hydrocarbon gases (acetylene, ethylene, methane) or liquid aliphatic saturated hydrocarbons, over metal catalysts supported on silica, alumina or zeolite at temperatures between 500 and 1000 °C. The catalyst consists of nano-sized particles of a single metal (Fe, Co or Ni) or a mixture of metals. CCVD has been reported to be a low cost method in producing multiwall carbon nanotubes and nanotube bundles. Another interesting aspect is the ability to induce the tube growth in a given direction with a control of the dimensions affected by the experimental conditions (nature of the catalyst, type of support, carbon source, temperature).

Composites obtained by dispersing nanotubes into different polymeric matrices have attracted wide attention in order to develop ultra-lightweight and extremely strong materials. In polymer composites, filler dispersion as well as interfacial interactions have been shown to be crucial parameters for enhanced mechanical properties. In fact, one of the biggest challenges is to obtain a homogeneous dispersion of carbon nanotubes in a polymer matrix because van der Waals interactions between individual tubes often lead to significant aggregation or agglomeration, thus reducing the expected property improvements of the resulting composite. But to date, despite the fact that much progress has been made in the processing techniques, the mechanical improvement brought about by incorporation of nanotubes remains minor with regard to the potential based on the properties of the nanotube itself. A review of Thostenson et al. [43] and Moniruzzanam and Winey [44] illustrates the significant challenges that must be overcome before the potential is realized.

Different techniques to attempt to optimize the nanotube dispersion within the polymeric medium have been used. They include solution mixing [45], sonication [46,47], coagulation [48], melt compounding [49–51], in situ miniemulsion polymerization [15,52,53], oxidation [54] or chemical functionalization of the tube surface [55–57], use of surfactants [58]. The ultimate goal of these processing conditions is to separate the individual nanotubes in order to get a homogeneous dispersion throughout the matrix while the chemical functionalization is intended to bring some adhesion between the nanotubes and the polymer thus enabling effective stress transfer at the polymer–filler interface.

Various strategies for chemical functionalization of carbon nanotubes have already been reported. They involve covalent or noncovalent attachments of functional groups in order to improve solubility and processability of CNTs in organic media. The use of ball milling in specific atmosphere allowed the introduction of functional groups such as thiol, amine, amide, chloride, carbonyl, thiomethoxy and acyl chloride, onto carbon nanotubes [59]. Functionalization of SWNTs via electrochemical reduction of a variety of aryl diazonium salts was described [60]. Functionalization can also be carried out

through oxidation of the nanotubes to induce formation of carboxylic, carbonyl or hydroxyl groups to nanotube end-caps or sidewalls. These functionalities serve as anchoring sites and open the way to further derivatization reactions that made the nanotubes soluble in organic solvents. For example, CNTs functionalized by oxidizing acid treatment can be submitted to fluorination and subsequent derivatization or to amine reactions with alkylcarboxyl groups attached to the nanotubes [61–64]. These types of approaches were successfully applied for the synthesis of epoxy matrices in which the nanotubes were integrated into the structure of the epoxy system through the sidewall amino functional groups [62,63]. Water-soluble SWNTs, interesting for chemical and biomedical applications, were also obtained by grafting glucosamine after producing acyl chloride on acid-treated nanotubes [65].

Functionalization via vigorous oxidation processes followed by covalent bonding has been shown to introduce defect sites within the nanotube structure where sp^2 hybridization is converted to sp^3 hybridization, which may affect the properties of the nanotube itself [66]. Electrochemical modification [67,68], surface-initiated polymerization in which polymer chains are covalently coupled onto the CNT surface which bears polymerization initiators [69–71] have been used to minimize damage of CNTs. On the other hand, shortening and mechanical damage such as buckling, bending and dislocations in the carbon structures were also induced by the sonication technique used to disperse the CNTs [72,73]. Shortening the nanotubes could be detrimental since it reduces the high aspect ratio which is one of the potential advantages of the nanotubes for their use as reinforcing fiber in polymer matrices.

3. Characterization of carbon nanotubes

The morphology and state of dispersion of the carbon nanotubes in a polymer matrix can be investigated using transmission electron microscopy (TEM) and atomic force microscopy (AFM).

Shown in Fig. 1 are typical TEM images of a toluene suspension of multiwall carbon nanotubes (MWNTs) previously sonicated before being put onto copper grids for observation (Fig. 1A–D). Fig. 1A reveals a broad distribution in lengths and diameters which are in the range of 0.1–5 μm and 10–50 nm, respectively, and Fig. 1B shows the curled structure of an individual tube. The nanotubes can be highly entangled with one another and form an interconnecting structure (Fig. 1C). Fig. 1D magnifies the nanostructure of a multiwall carbon nanotube with several layers of graphitic carbon and a hollow core.

Fig. 1E–H shows the TEM images of composite based on styrene–butadiene rubber (SBR) filled with 4 phr of MWNTs (phr = parts per hundred parts of rubber). Bundled MWNTs can be clearly identified in Fig. 1E. Individual nanotubes are visualized in Fig. 1F and G and black spots correspond to aggregates. A magnification of one bundle (Fig. 1H) shows an orientation of nanotubes occurring probably during hot pressing of the film. This orientation is expected to play a role in mechanical reinforcement.

TEM images were obtained on a JEOL 100CXII. Pure carbon nanotubes were sonicated in toluene and droplets of the suspension were put onto copper grids for observation. Ultrathin films (60 nm thick) of the composite samples were cut by means of an ultramicrotome LEICA ULTRACUT UCT cooled at −80 °C by liquid nitrogen and put onto copper grids.

Additional information on how the nanotubes are actually being distributed within the polymer matrix can be obtained from atomic force microscopy. AFM has been shown to be particularly well suited for the characterization of filled elastomers and more generally of heterogeneous systems with components of different stiffness [74].

AFM images of SBR filled with 10 phr of MWNTs, shown in Fig. 2, give some indication of a larger scale dispersion than that given in Fig. 1. The brighter domains easily identified and rather homogeneously distributed in the film, are ascribed to filler aggregates. It has to be recalled that topography and error signal reveal surface roughness while phase imaging, which provides variation of surface stiffness, is particularly useful in elastomeric composites filled with carbon nanotubes on account of huge differences in moduli between the two components.

AFM investigations were performed with a Thermomicroscope CP Research System, using tapping mode and phase imaging. Topography, error signal and phase images were simultaneously recorded in order to get a topographic and compositional mapping of the surface.

4. Mechanical properties of nanotube-based elastomeric composites

Conventional fillers such as carbon black or silica, when added to elastomeric systems usually cause an increase in the modulus involving a hydrodynamic effect arising from the inclusion of rigid particles and an increase in the cross-linking density created by polymer–filler interactions [75–81].

The anisometry of particle aggregates or agglomerates is also expected to increase the modulus as well as the occluded rubber, considered as a typical mechanical interaction and consisting of elastomer chains trapped inside the filler aggregates. This occluded rubber, which is assumed to be partially shielded from deformation, increases the effective filler concentration.

The extent of filler agglomeration has a marked influence on the low strain dynamic properties of filled vulcanizates. While unfilled elastomers display little changes in dynamic properties upon increasing strain amplitude, the storage modulus of filled systems decreases significantly showing a typical non-linear behavior known as the Payne effect [82]. A large amount of work has been reported on this effect but the most accepted interpretation is the gradual breakdown of the filler network or filler ''networking'' as denominated by Wang [83], with increasing strain amplitude. In his paper reviewing the effect of filler characteristics on dynamic properties in connection with processing conditions and additives,

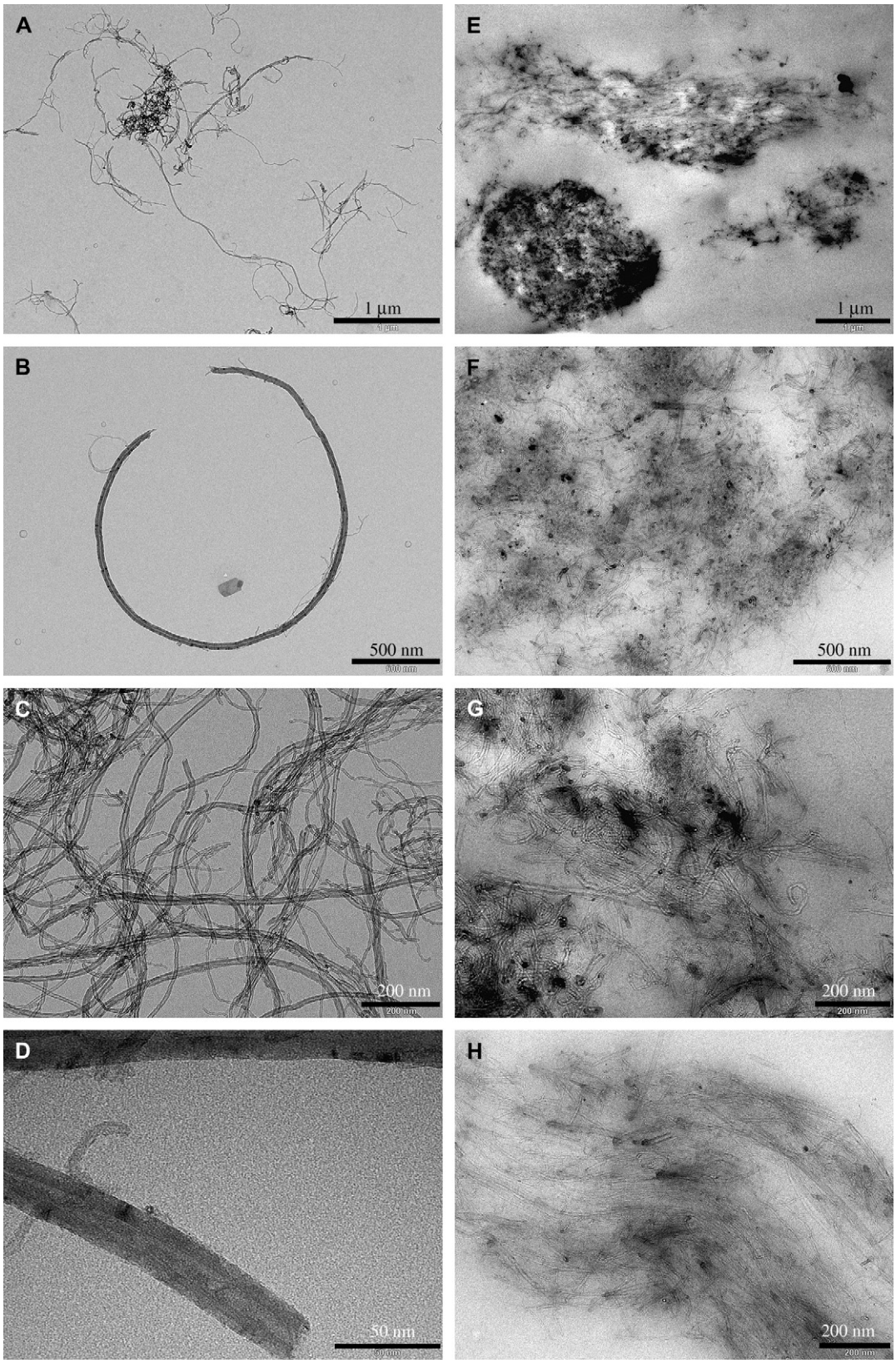

Fig. 1. TEM images. A–D: pure MWNTs; E–H: SBR/4 phr MWNT composite.

Wang demonstrates that the formation of the filler network is not only the result of filler–filler interactions but also of polymer–filler and polymer–polymer interactions. Nevertheless any processing method improving dispersion and avoiding the formation of direct inter-particle contacts or increasing the polymer–filler interactions will depress filler networking.

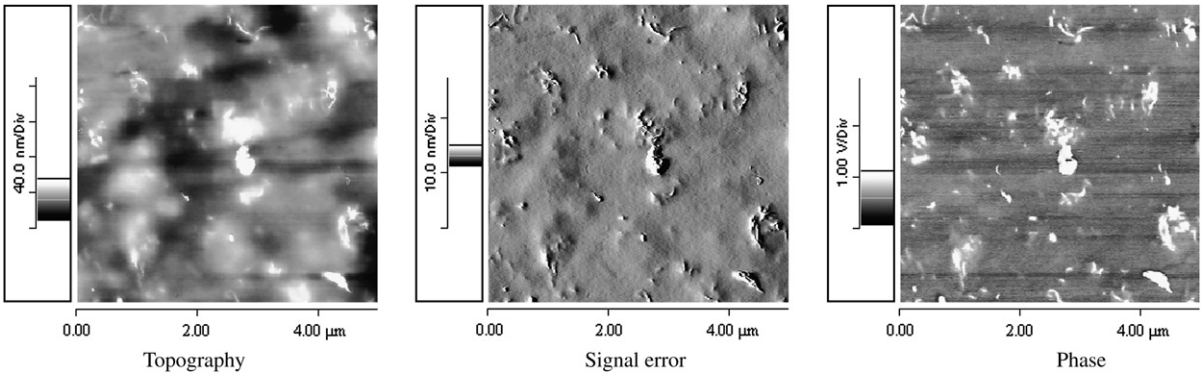

Fig. 2. AFM images of SBR filled with 10 phr of multiwall carbon nanotubes (MWNTs).

Also related to reinforcement is the stress-softening effect called the ''Mullins effect'', observed at high extensions and characterized by a pronounced lowering in the stress when the filled vulcanizate is extended a second time [84]. This process, which can be considered as a hysteretic mechanism related to energy dissipated by the material during deformation, corresponds to a decrease in the number of elastically effective network chains. It results from chains that reach their limit of extensibility by strain amplification effects caused by the inclusion of undeformable filler particles [85,86]. Stress-softening in filled rubbers has been associated with the rupture properties and a quantitative relationship between total hysteresis (area between the first extension and the first release curves in the first extension cycle) and the energy required for rupture has been derived [87,88].

On account of their extremely high moduli, carbon nanotubes are expected to provide much higher reinforcement effects than conventional fillers. By using an atomic force microscope, Salvetat et al. [89] measured elastic moduli of SWNTs around 1 TPa and with a technique based on electrically induced mechanical deflections of MWNTs in a transmission electron microscope, instead of; elastic bending modulus was found to decrease sharply (from about 1 to 0.1 TPa) with increasing diameter (from 8 to 40 nm) [90]. On the other hand, tensile strengths of individual MWNTs were measured with a ''nanostressing stage'' located within a scanning electron microscope [91]. It was shown that the MWNTs broke in the outermost layer and the tensile strength of this layer ranged from 11 to 63 GPa while the Young's modulus varied from 270 to 950 GPa.

Significant improvements in mechanical properties of polymeric matrices by CNT addition have been reported. Allaoui et al. [92] found that the incorporation of 1 wt.% of MWNTs into an epoxy matrix results in an increase in the Young's modulus and in the yield strength by, respectively, 100 and 200% compared to the pure matrix. Reinforcement effects were also observed by adding MWNTs in phenolic resins [93,94] and in polystyrene [95]. Nevertheless, in polyethylene composites, McNally et al. [96] observed a decrease in the ultimate tensile strength and elongation at break with addition of MWNTs suggesting poor interfacial interactions between the MWNTs and the polymer matrix.

Some studies also report the use of CNTs in elastomeric matrices. SWNTs [17] and MWNTs [97] were incorporated in natural rubber. In the first paper, the reinforcing effect of the nanotubes is revealed by a dynamic mechanical analysis showing an increase in the storage modulus. In the second paper, tensile strength, tensile modulus and toughness are shown to increase with the filler loading while the elongation at break decreases. Tensile tests performed on a silicone rubber mixed with SWNTs also display dramatic improvement in the mechanical properties as a function of filler content [16]. The initial modulus increase has been shown to be approximately linear with weight fraction, with a slope of 200%/wt.%.

We have investigated the effect of incorporation of multiwall carbon nanotubes (MWNTs) into elastomeric matrices. The level of reinforcement is assessed through a mechanical characterization as a function of nanotube loading.

Fig. 3 shows, as a typical example, stress–strain curves for a pure styrene–butadiene rubber (SBR) and for MWNTs/SBR composites and the experimental mechanical properties are listed in Table 1. The styrene–butadiene rubber contains

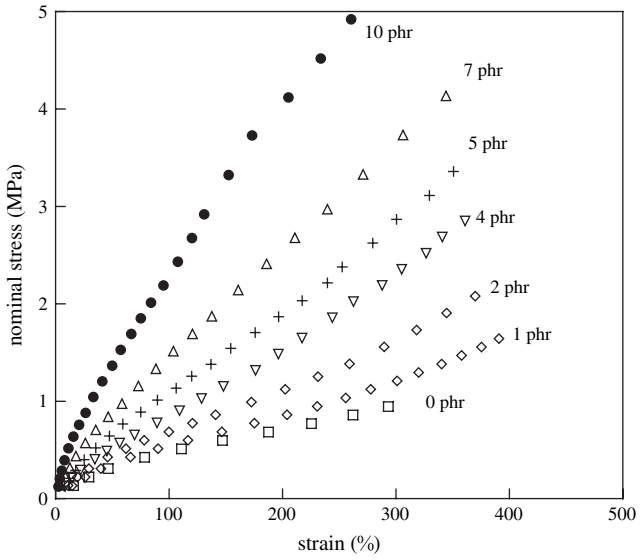

Fig. 3. Stress–strain curves for pure SBR and MWNT/SBR composites. The filler content is expressed in phr (phr = parts per hundred parts of rubber).

Table 1
Mechanical properties of SBR and SBR composites

Filler loading (phr)	E (MPa)	Stress at 100% (MPa)	Stress at 200% (MPa)	Stress at 300% (MPa)	Stress at break (MPa)	Strain at break (%)	Q_{rubber}
0	0.24	0.49	0.71	0.96	0.95	300	6.54
1	0.35	0.55	0.85	1.21	1.64	390	5.99
2	0.43	0.70	1.10	1.62	2.08	370	5.59
3	0.59	0.89	1.46	2.11	3.13	420	4.92
4	0.61	0.86	1.51	2.32	2.85	360	4.83
5	0.73	1.11	1.89	2.84	3.36	350	4.64
7	0.93	1.48	2.54	3.67	4.14	350	3.81
10	1.40	2.44	3.91	–	4.92	260	3.15

Q_{rubber} represents the equilibrium swelling ratio of the rubber phase in toluene.

25 wt% of styrene units. The microstructure of the butadiene phase is the following: 10% *cis*, 17% *trans*, 73% 1,2.

The strain–stress measurements were carried out at room temperature on strips of $50 \times 5 \times 0.2\ mm^3$ between two clamps by means of a sequence of increasing weights attached to the lower clamp. The distance between two marks on the sample was measured with a cathetometer after allowing sufficient time (10 min after adding a weight) for equilibration.

Clearly there is reinforcement as evidenced by considerable improvements in stiffness and tensile strength of the composites with the filler loading. With the addition of only 1 phr of MWNTs (phr = parts per hundred parts of rubber), a 45% increase in elastic modulus and a 70% increase in the tensile strength are achieved. The slight reduction in the ultimate strain observed for the sample filled with 10 phr of MWNTs with regard to the pure polymer may result from the presence of aggregates increasing with the filler content.

As these systems are submitted to sulfur vulcanization, SH-functionalized MWNTs were also used in order to determine whether the grafted groups are involved in the vulcanization process, thus bringing some adhesion between the organic and inorganic phases. No further improvement in the mechanical properties is gained with regard to the results obtained with untreated carbon nanotubes which is probably due to the small degree of nanotube functionalization which is around 1%. In a recent paper of Miltner et al. [98] dealing with nanocomposites based on ethylene–vinyl acetate copolymer in combination with several types of organoclay or carbon nanotubes, chemically functionalized carbon nanotubes bearing acetate or hydroxy moieties at their surface are seen to display less interactions than clay-filled systems at similar loading. The authors also mention the limited degree of surface functionalization.

The extent of reinforcement depends on several filler characteristics such as its modulus, geometry and orientation within the host matrix [99,100]. The extremely high modulus of carbon nanotubes (the value of 1 TPa is usually reported in the literature) may provide composites with mechanical properties that exceed those of any previously existing materials. On the other hand, according to theories and models describing the tensile behavior of filled composites, fibers are the most efficient at enhancing stiffness [101]. In order to take advantage of the full potential of carbon nanotubes for any given application in polymer nanocomposites and to understand their superior efficiency as reinforcing fillers, it is interesting to compare the experimental data with theoretical models intended to predict the properties of composite materials. The Guth model [102] only based on the aspect ratio, f, and volume fraction, ϕ, of filler, has been widely used to account for the change in modulus in filled elastomers:

$$E = E_0\left(1 + 0.67f\phi + 1.62f^2\phi^2\right), \tag{1}$$

E and E_0 are the moduli of the composite and the unfilled elastomer, respectively.

The Halpin–Tsai model [103] also predicts the stiffness of the composite as a function of the aspect ratio. The longitudinal modulus measured parallel to perfectly oriented fibers is expressed in the general form:

$$E = E_0(1 + 2f\phi\eta)/(1 - \phi\eta) \tag{2}$$

where η is given by

$$\eta = \left[\left(E_f/E_0 - 1\right)/\left(E_f/E_0 + 2f\right)\right] \tag{3}$$

E_f being the modulus of the filler.

In elastomeric composites, $E_f \gg E_0$, so Eq. (2) reduces to

$$E = E_0(1 + 2f\phi)/(1 - \phi) \tag{4}$$

In Fig. 4, the experimental values of E/E_0 are compared with the Guth and Halpin–Tsai predictions using the respective aspect ratios of 40 and 45 to fit the data. While the Guth model departs from the experimental results at the highest filler loadings, the Halpin–Tsai model, for perfectly aligned fibers, shows good agreement within the volume fraction range investigated. It is interesting to mention that both models yield almost similar aspect ratios. The values required to fit the experimental data are lower than that calculated from the average dimensions of the MWNTs. It is most probably due to aggregation of the nanotubes which reduces the aspect ratio of the reinforcement.

As already mentioned, nanotube alignment occurring, partially during film processing or, of course during stretching, has to be taken into account in the mechanical behavior of the composites. Phase-contrast tapping-mode AFM imaging of silica-filled elastomers under uniaxial stretching has greatly improved our molecular understanding of rubber reinforcement [104]. AFM observation of carbon nanotube-filled SBR was also carried out in order to have a look at the behavior

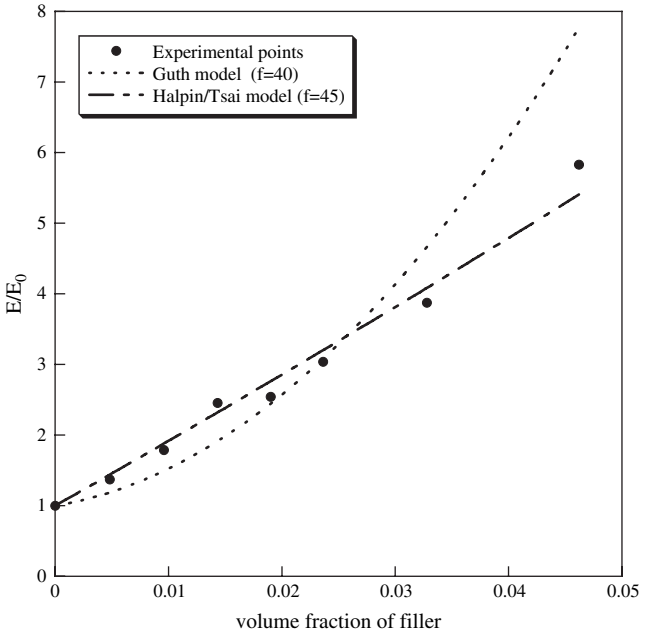

Fig. 4. Experimental moduli plotted versus volume fractions of MWNTs and comparison with theoretical predictions.

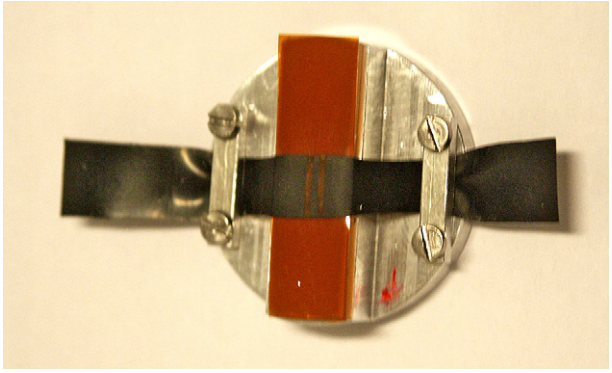

Fig. 5. Stretching device for AFM experiments.

of filler aggregates upon application of a macroscopic strain and also after suppression of the strain and second stretching. The sample (around 200 μm thick) was put on a small stretching device specially fitted to the sample holder of the multimode AFM (Fig. 5). The deformation is maintained, thanks to the clamps screwed in the body of the device. The strain can be evaluated from the measurement of the distance between the two ink lines drawn on the surface of the film.

Phase images of films stretched to extension ratio (ratio of the length of the sample in the direction of strain to the initial length before deformation) equal to 1.8 and then 2.8 are shown in Fig. 6 for the 10 phr filled composite. Applying a uniaxial deformation to the sample results in orientation of the filler aggregates appearing as white areas. At the highest elongation, the bundles can be seen to be broken up into long straight structures. A quite different morphology is obtained after relaxation of the sample to the unstressed state (Fig. 7a) which is in fact more deformed than the original material on account of the permanent deformation exhibited by filled elastomers. In the relaxed sample, the data suggest a rotation of domains and an orientation of the bundles perpendicular with the stress direction. A second stretching at an extension ratio of 2.3 has not the same effect as that performed on the original material.

Another indirect evidence of chain orientation induced by tube alignment has been obtained by infrared analysis of stretched MWNT-filled natural rubber. Natural rubber is able to crystallize under strain, a phenomenon that can be followed by infrared spectroscopy where it is seen that the band associated with the C–H out-of-plane vibration, located at 837 cm^{-1} in the isotropic state shifts to higher wavenumbers upon crystallization (Fig. 8a). The change in wavenumber upon uniaxial stretching is observed at a lower extension ratio for the composite thus showing that the strain-induced crystallization process occurs at a lower deformation in the presence of carbon nanotubes as a result of a stronger orientation of polymer chains induced by alignment of filler bundles (Fig. 8b). This

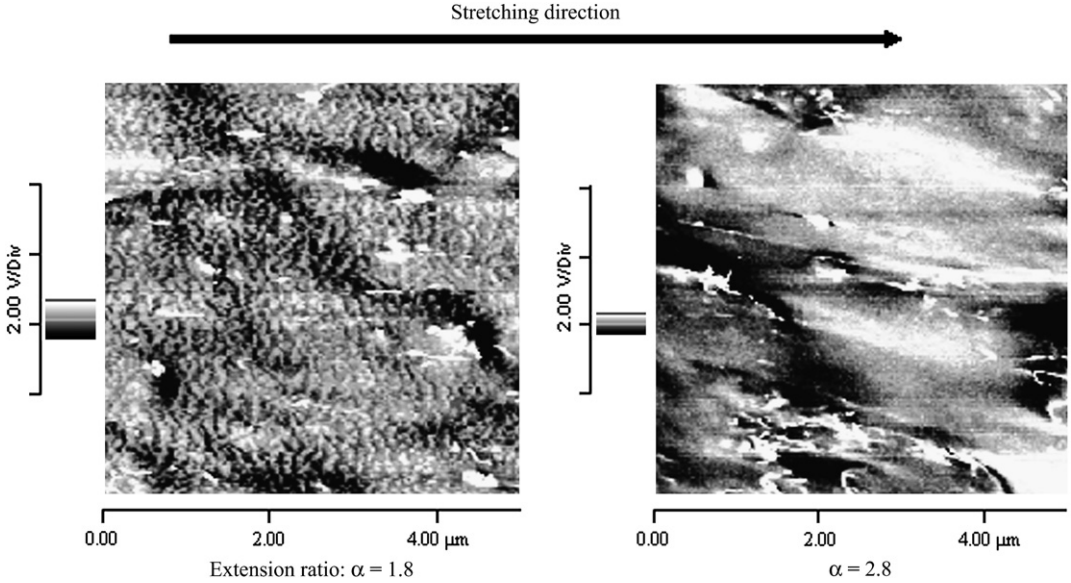

Fig. 6. Tapping-mode AFM phase-contrast images (5 μm × 5 μm) for the 10 phr MWNT-filled SBR under two different elongations.

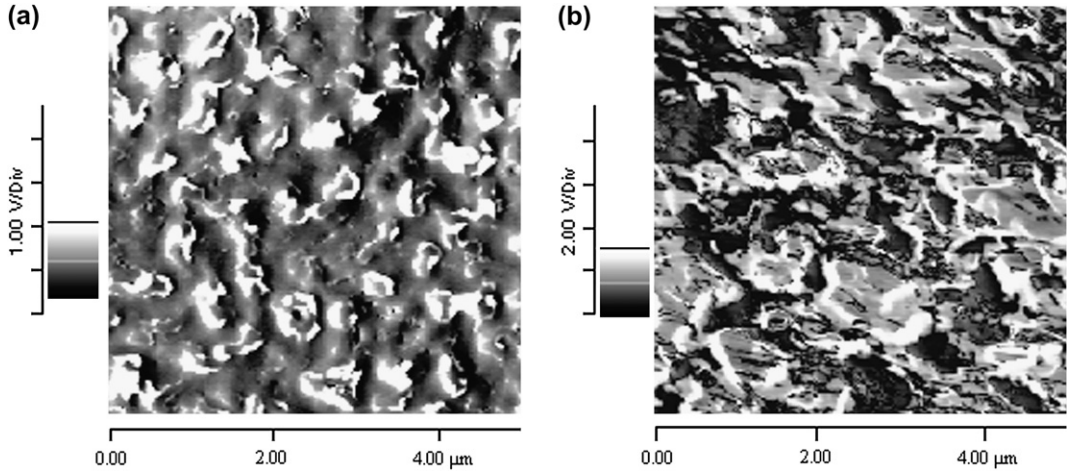

Fig. 7. AFM images after total release of the stress (a) and subsequent stretching at $\alpha = 2.3$ (b).

interpretation which is speculative needs to be confirmed by further investigations on stretched systems.

5. Experimental evaluation of the interactions between carbon nanotubes and elastomers

Most of the theoretical models predicting the elastic modulus of filled rubbers assume uniform dispersion and perfect adhesion between the polymer and the matrix. TEM analysis of the composites has revealed a poor dispersion. On the other hand, the existence of interfacial interactions between the nanotubes and the matrix, which is critical in mechanical reinforcement, is not obvious. The strong restriction in equilibrium swelling in toluene with the MWNT content (Table 1) would suggest that a certain polymer–filler bonding or a state of adhesion between the two phases is established. But a more realistic interpretation of the swelling deficit in the presence of carbon nanotubes would be the occlusion of rubber into the aggregates. During processing, carbon nanotubes are well dispersed in toluene solution and then reagglomerate after incorporation of polymer thus entrapping elastomer molecules which behave like filler and do not swell [105]. On the other hand, some hysteresis (area between the first stretch and the second stretch) has been observed at large strains for the samples filled with MWNTs (Fig. 9). After stretching and release, the sample exhibits a large degree of permanent deformation. The hysteresis, also called ''stress-softening effect'' has been shown to correspond, in the case of conventional composites, to a loss of elastic chains taking place at the polymer–filler interface [86]. It is very low in the case of poor polymer–filler interactions [106]. In view of the AFM observations, we are in a position to believe that in carbon nanotube-filled samples, the stress–strain behavior of the composites contains a large contribution arising from orientational effects and that the pronounced lowering in the stress observed in the second stretching corresponds to a loss of orientation once the stress is released.

Dynamic mechanical analysis measurements were performed on pure natural rubber (NR) and composites with up to 10 phr of MWNTs. The temperature dependence of the

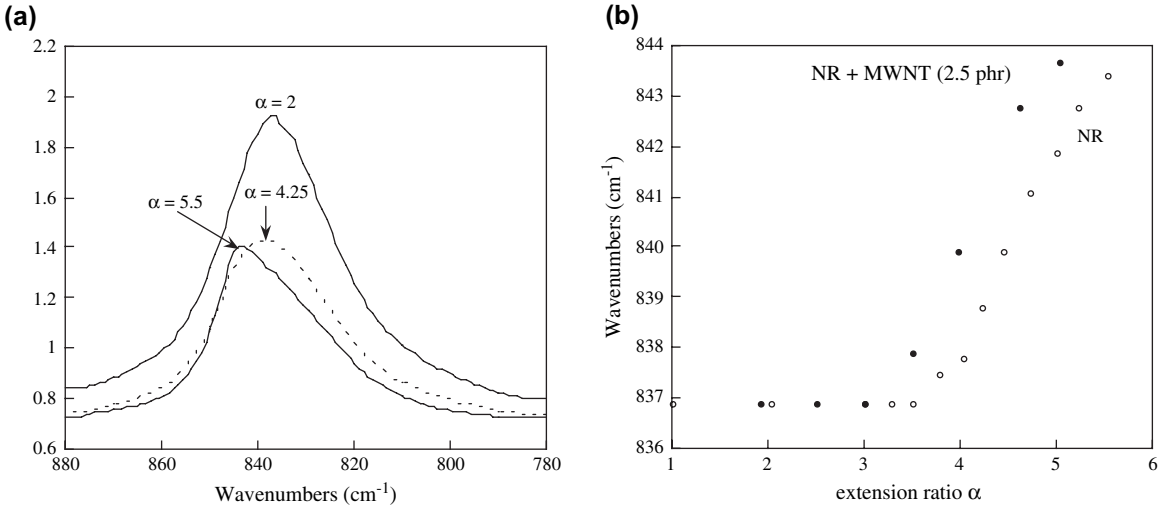

Fig. 8. Shift of the C–H out-of-plane absorption band upon crystallization of unfilled natural rubber (a) and dependence of its wavenumber on the extension ratio α (b).

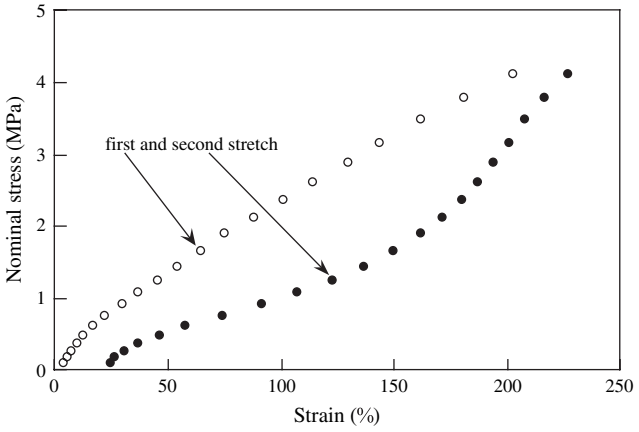

Fig. 9. Mullins hysteresis for the SBR/10 phr MWNT composite.

storage modulus G' and of the loss factor tan δ for the unfilled and 10 phr MWNT-filled NR are reported in Fig. 10. Around −60 °C, the storage modulus G' decreases abruptly while tan δ passes through a maximum. This relaxation process is of course related to an energy dissipation associated with the glass transition phenomenon of the rubber phase. As seen in Fig. 10, the glass transition temperature taken at the maximum of tan δ does not change significantly upon incorporation of the nanotubes in the matrix, since the T_g values increases from −61.3 °C for pristine NR to −59.8 °C for the filled sample. This small effect of MWNTs on the glass transition temperature of the rubber cannot be a sign of a lack of adhesion of the filler to the elastomer since several authors have reported little influence of the presence of carbon blacks on T_g even at high filler loading and with reinforcing blacks [82].

In conventional composites, the adsorption of polymer molecules gives rise to the formation of an adsorption layer, evidenced by dielectric or solid state NMR spectroscopies [5,107], whose thickness has been estimated around 2 or 3 nm and where motions of chain units are more restricted than those in the mobile phase. The loss in segmental mobility would result in an increase in T_g and most probably in a change of the thermal expansion of the free volume. Surprinsingly, investigations carried out on a styrene–butadiene copolymer

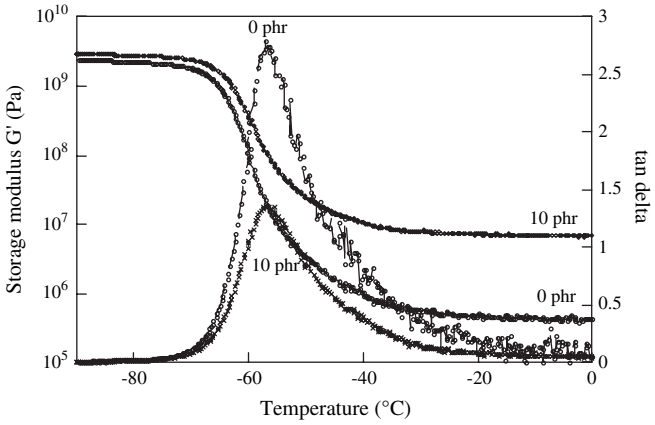

Fig. 10. Temperature dependence of the storage modulus and of the loss factor for pure NR and NR/10 phr MWNT composite.

filled with different carbon blacks, show that T_g is only increased by about 1 °C by every 50 phr of highly reinforcing filler but remains unaffected by relatively inert carbon black while the coefficient of expansion of the polymer component of the composite is substantially unaffected by all carbon blacks in the rubbery region [108].

For composites of poly(methyl methacrylate (PMMA) and unmodified SWNTs tan δ peak broadens but the peak is at the 105 °C value of bulk polymer for the unfunctionalized composite while the amide-functionalized PMMA composite displays a tan δ peak shifted to a higher temperature by 30 °C with regard to the pure polymer [56]. The amide-functionalized PMMA composite displays a tan δ peak shifted to a higher temperature by 30 °C with regard to the pure polymer. The authors suggest the existence of discrete interphase regions with unmodified SWNTs due to clustering of tubes while the functionalized composite system has a stronger interfacial bonding via the covalent linkages between the two phases leading to the formation of an extensive region with altered properties. From SEM analysis of MWNT/polycarbonate composites, Pötschke et al. [109] and Ding et al. [110] observed tube diameters larger than those of the pristine MWNTs used in the sample preparation and suggest the existence of an adsorbed layer of polymer on the tubes' surface but unfortunately do not mention if a shift in T_g is associated with the tube coating. Additionally, a dependence of the nanotube content on the glass transition temperature was observed for MWNT/epoxy composites with a stronger increase in T_g for samples containing amino-functionalized nanotubes [55]. The authors do not exclude a possible effect of the additional functional groups on the curing reaction of the epoxy matrix.

As seen in Fig. 10, at higher temperatures, the storage modulus reaches a plateau around 0.3 MPa at 20 °C for the unfilled NR and 6.2 MPa for the composite. This large modulus increase in the rubbery plateau, which represents the reinforcement provided by the carbon nanotubes, is much higher than that obtained in the tensile mechanical characterization because it includes the contribution arising from filler–filler interactions. This contribution is usually evidenced through the strain dependence of the storage modulus. Reinforced elastomers and more generally systems containing filler dispersions are characterized by a non-linear viscoelastic behavior, known as the "Payne effect" [111,112]. With regard to the unfilled rubber, the composite containing 10 phr of MWNTs has been shown to display a greater Payne effect probably associated with the breakdown of large agglomerates of carbon nanotubes (Fig. 11).

Interactions between the nanotube bundles and the matrix are required for an efficient stress transfer from the matrix to the nanotubes. Raman spectroscopy has proved to be very sensitive for an evaluation of the strength of the polymer–filler interface. In fact, carbon nanotubes exhibit well-defined Raman peaks located for our MWNTs at 1345, 1595 and 2700 cm^{-1}, respectively, assigned to the disordered graphite structure (D band), tangential stretching mode of carbon–carbon bonds (G band) and to the overtone of the D band (G′ band) (Fig. 12). Cooper et al. [113] have shown that the G′ band shifts to a lower wavenumber upon application of a tensile stress on

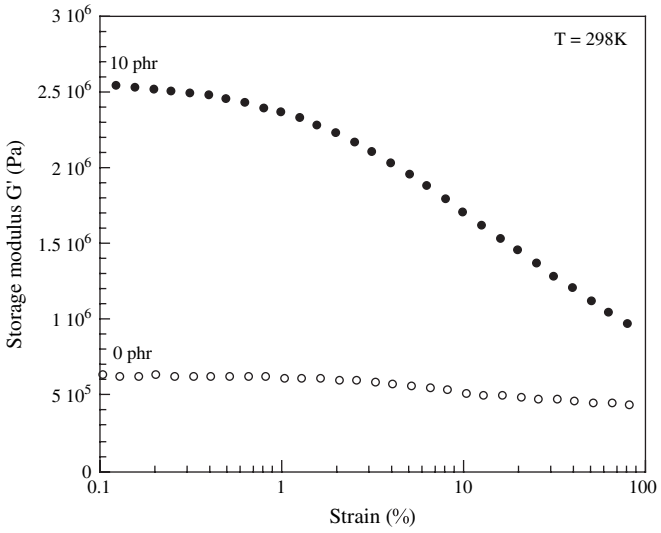

Fig. 11. Strain dependence of the storage modulus for pure NR and NR/10 phr MWNT composite.

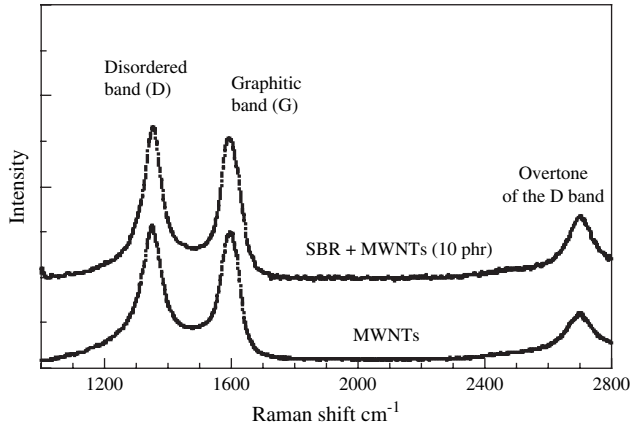

Fig. 12. Raman spectra of pure MWNTs and SBR/MWNT composite at 514 nm excitation. Intensities of the spectra have been adjusted to improve presentation.

composites based on epoxy resins and single or multiwall carbon nanotubes. According to the authors, this shift indicates stress transfer from the matrix to the nanotubes and hence reinforcement. Nevertheless, the rates of band shift were found to differ for all the nanotubes investigated. Poorer dispersion, worse adhesion and lower aspect ratio were invoked to account for smaller shift rate. In our case, the Raman peaks were not found to shift when the composite is subjected to an extensional strain, indicating weak interfacial interactions.

6. Electrical properties

In addition to improving the mechanical properties, black fillers (carbon black or carbon nanotubes) impart conductivity to low resistivity elastomeric matrices. In many applications, electrical conductivity is required to dissipate electrostatic charge. The electrical properties are strongly affected by the filler concentration, the filler morphology such as particle size and structure as well as filler–filler and filler–matrix interactions which determine the state of dispersion. Nanotube orientation will also influence the electrical conductivity. There is a critical volume fraction known as the percolation threshold at which the conducting inclusions form an interconnecting filler network leading to a sharp drop in the electrical resistance.

Fig. 13 shows the effect of filler loading on the volume resistivity of carbon black (N330 from Cabot) (CB) and MWNT-filled composites based on insulating styrene–butadiene rubber. Electrical resistivity measurements were determined on samples of $10 \times 20 \times 0.2\ \mathrm{mm}^3$ by measuring their resistance on a high resistance meter (Keithley 6517A) between two conductive rubber electrodes with an alternative voltage of 1 V. This alternative voltage is needed to avoid a background current effect. The measured resistances R were then converted into volume resistivity ρ using the following equation:

$$\rho = \frac{RS}{d} \tag{5}$$

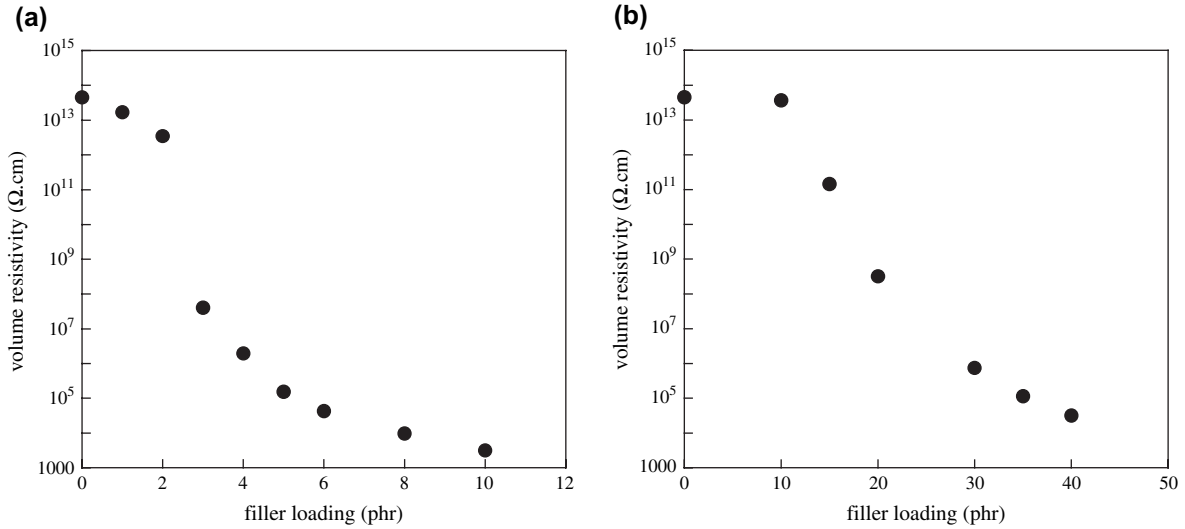

Fig. 13. Volume resistivity against filler loading for SBR composites filled with MWNTs (a) or CB (b).

where S is the cross-sectional area perpendicular to the current and d is the thickness of the sample between the two electrodes.

The continuous network is formed at a lower filler loading of the nanotube bundles with MWNTs than with CB. The higher aspect ratio of the nanotube bundles which increases the probability of particle–particle contacts explain the low percolation threshold. Our results are in agreement with those of Flandin et al. [114] and of Thongruang et al. [115] who showed that the percolation-threshold concentration in composites is around 10–15 wt.% for carbon fiber and high structure carbon black and around 40–50 wt.% for low structure carbon black and graphite. The high electrical conductivity of carbon nanotube-filled composites obtained at a relatively low volume fraction is one of the major attributes of carbon nanotubes since that allows to retain the desired mechanical properties. The higher loadings of carbon black, required to provide the same level of conductivity, often lead to an increase in viscosity and consequently to a reduction and processing ease and can be associated with a reduction in mechanical properties.

Since the resistivity of the unfilled elastomer is several orders of magnitude larger than that of the filled vulcanizate, any rearrangement of the filler particle distribution induced, for example, by application of a deformation, leads to a change in the vulcanizate conductivity. Significant changes in electrical resistivity against deformation in black-filled composites have already been reported in the literature [114,116–121]. At small deformations, changes in dynamic moduli with strain amplitude have been found to be very similar to changes in conductivity with strain amplitude [116–118]. The storage modulus, G' and the dynamic conductivity have been shown to decrease in a similar way as the amplitude of dynamic oscillation was increased. The reduction of both conductivity and modulus has been associated with the breakdown of the carbon network.

Here, is considered, the effect of a uniaxial deformation on the electrical properties of a material whose MWNT concentration is above the insulator–conductor transition region. To measure changes in resistivity, strips (size: $50 \times 15 \times 1\ mm^3$) were stretched with a manual stretching machine in which two clamps connected to the high resistance meter, were placed along the length of the specimen (Fig. 14).

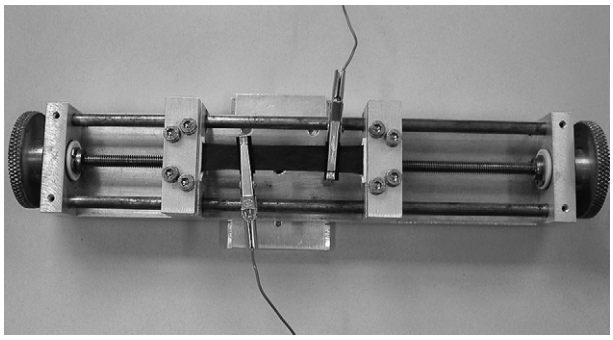

Fig. 14. Stretching machine for electrical measurements under uniaxial extension.

Measurements were made at about 5 mn after each elongation step. Static resistance, R, of the vulcanizate under uniaxial extension was measured in the direction of strain and the resistivity, ρ, was calculated from the following expression:

$$\rho = \frac{RS}{L} = \frac{RS_0}{\alpha^2 L_0} \tag{6}$$

where S_0 and L_0 are, respectively, the initial cross-sectional area and length between the two clamps before deformation and α is the extension ratio. Under uniaxial extension, the deformed length, L, becomes αL_0 while S is equal to S_0/α, if the volume remains constant during deformation.

The change in resistivity during uniaxial extension for a composite filled with 10 phr of MWNTs is shown in Fig. 15. It is observed that the resistivity of the sample increases gradually with the applied strain. Our results differ from those presented by Yamaguchi et al. [121] for carbon black-filled elastomers where an increase in resistivity at low strains is observed, followed by a subsequent reduction at higher extensions. The authors explain the rise in the initial resistivity by a breakdown of carbon black agglomerates into smaller aggregates and consequently a reduction in the total number of conduction paths. They attribute the subsequent reduction to the orientation of the carbon black aggregates in the direction of strain. Das et al. [120] observed, for carbon black and short carbon fiber filled rubber composites, that the resistivity increases rapidly with the degree of elongation strain and explain the increase in resistivity by a breakdown of existing conductive networks and formation of new conductive networks by rearrangements and orientation of black particle aggregates or fibers. Donnet and Voet [118] consider that the strain dependence of the electrical properties of carbon black-loaded vulcanizates can be interpreted at small extensions by the reversible formation and destruction of the transient carbon network, up to 150% extension by an orientation of carbon

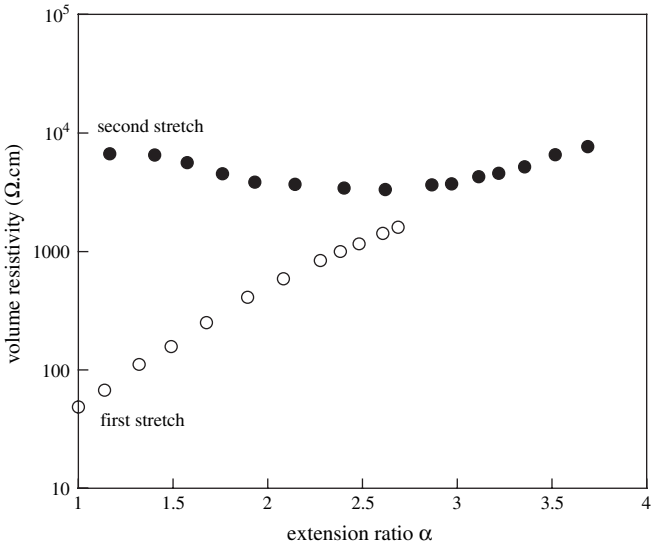

Fig. 15. Dependence of the electrical resistivity on the extension ratio α for the SBR/10 phr MWNT composite.

black aggregates and to rupture of elastomer–carbon bonds at still higher extensions.

According to our AFM experiments under strain, we ascribe the gradual increase in resistivity with strain (Fig. 15) to the orientation of the nanotube bundles rather than to the destruction of large filler structures. Our interpretation is in agreement with the results of Du et al. [48] who showed that alignment of a nanotubes worsens the electrical conductivity and also shifts the percolation threshold.

In order to parallel the mechanical measurements, electrical measurements are also carried out during a second stretching performed 1 h after total unloading of the sample.

After total unloading of the sample, as already reported in other studies [120,121], the resistivity of the fully relaxed composite is significantly higher than that measured in the unstrained elastomer showing that the filler network is not re-formed after removal of the stress. During the second stretching performed 1 h after retraction, the resistivity slightly decreases on account of a reformation of new conductive contacts. When the strain reaches the maximum value of the first stretching, the two curves coincide which means that the sample is in the same state as it was at the first stretching. In light of the AFM experimental observations, we can ascribe the strong hysteresis in the conductivity–strain curve to rearrangements and disorientation of the bundles.

7. Conclusion

In this review, results obtained on carbon nanotube reinforced polymers are presented. While the polymeric media are focused on elastomeric matrices, results obtained on other materials are also mentioned when needed in the discussion.

After a brief presentation on the synthesis methods and processing of nanotube-based polymer composites, the factors expected to control their mechanical properties are discussed in relation to what is already known on composites filled with conventional fillers such as carbon black or silica. Specific features of carbon nanotubes related to their modulus, geometry and orientation, are also taken into account. In particular, atomic force microscopy imaging under uniaxial extension of the sample gives evidence of the contribution of the orientational effects.

Poor dispersion and lack of interfacial adhesion between the tubes and the polymer are limiting factors for full realization of filler capability. Up to now, the improvements in mechanical properties of the neat polymer by carbon nanotube incorporation remain modest with regard to what should be expected from a nanometer-scale reinforcement. This demonstrates the need for optimizing the processing conditions to achieve good dispersion and good interactions with the polymer chains. This could be done by an appropriate functionalization of the tube surface or by introducing in the medium a type of coupling agent able to react with both phases. On the other hand, a method of incorporating simultaneously carbon nanotubes and another type of filler, namely carbon black particles, could be of interest on account of possible synergistic effects that could arise between the two different fillers. Through a combination of benefits of each type of filler, these hybrid composites could potentially exhibit improved characteristics with regard to single-filler materials. In particular, carbon black particles may improve the formation of connected structures by bridging uncontacted tubes.

The capability of carbon nanotubes to impart conductivity to insulating elastomeric matrices has been clearly shown. Electrical measurements carried out under uniaxial deformation display a gradual increase in resistivity as a result of a breakdown and an orientation of the filler particles.

In conclusion, this preliminary experimental work in carbon nanotube-based elastomeric composites has demonstrated the potential of this new form of carbon as a reinforcing filler of rubber materials. Most markedly, this work has illustrated the problems encountered with the dispersion and interaction in the host polymeric medium.

References

[1] Bokobza L. Macromolecular Materials and Engineering 2004;289:607.
[2] McCarthy DW, Mark JE, Schaffer DW. Journal of Polymer Science, Part B: Polymer Physics 1998;36:1167.
[3] McCarthy DW, Mark JE, Clarson SJ, Schaffer DW. Journal of Polymer Science, Part B: Polymer Physics 1998;36:1191.
[4] Kohjiya S, Murakami K, Iio S, Tanahashi T, Ikeda Y. Rubber Chemistry and Technology 2001;74:16.
[5] Dewimille L, Bresson B, Bokobza L. Polymer 2005;46:4135.
[6] Osman MA, Atallah A, Muller M, Suter UW. Polymer 2001;42:6545.
[7] Joly S, Garnaud G, Ollitrault R, Bokobza L. Chemistry of Materials 2002;14:4202.
[8] Varghese S, Karger-Kocsis J. Polymer 2003;44:4921;
Rubber World 2004;230:32.
[9] Kim J-t, Oh T-s, Lee D-h. Polymer International 2004;53:406.
[10] Arroyo M, López-Manchado MA, Herrero B. Polymer 2003;44:2447.
[11] Bala P, Samantaray BK, Srivastava SK, Nando GB. Journal of Applied Polymer Science 2004;92:3583.
[12] Jeon HS, Rameshwaram JK, Kim G. Journal of Polymer Science, Part B: Polymer Physics 2004;42:1000.
[13] Gauthier C, Chazeau L, Prasse T, Cavaillé JY. Composites Science and Technology 2005;65:335.
[14] Bokobza L, Chauvin J-P. Polymer 2005;46:4144.
[15] Barraza HJ, Pompeo F, O'rear EA, Resasco DE. Nano Letters 2002;2:797.
[16] Frogley MD, Ravich D, Wagner HD. Composites Science and Technology 2003;63:1647.
[17] López-Manchado MA, Biagiotti J, Valentini L, Kenny JM. Journal of Applied Polymer Science 2004;92:3394.
[18] Iijima S. Nature 1991;354:56.
[19] Bachtold A, Hadley P, Nakanishi T, Dekker C. Science 2001;294:1317.
[20] Derycke V, Martel R, Appenzeller J, Avouris Ph. Nano Letters 2001;1:453.
[21] Rotkin SV, Zharov I. International Journal of Nanoscience 2002;1:347.
[22] Akita S, Nishijima H, Nakayama Y, Tokumasu F, Takeyasu K. Journal of Physics D: Applied Physics 1999;32:1044.
[23] Cheung CL, Hafner JH, Odom TW, Kim K, Lieber CM. Applied Physics Letters 2000;76:3136.
[24] Wilson NR, Cobden DH, Macpherson JV. Journal of Physical Chemistry B 2002;106:13102.
[25] Yenilmez E, Wang Q, Robert RJ, Wang D, Dai H. Applied Physics Letters 2002;80:2225.
[26] Ye Q, Cassell AM, Liu H, Chao K-J, Han J, Meyyappant M. Nano Letters 2004;4:1301.
[27] Breuer O, Sundararaj U. Polymer Composites 2004;25:630.

[28] Wise KE, Park C, Siochi EJ, Harrison JS. Chemical Physics Letters 2004;391:207.
[29] Ajayan PM, Shadler LS, Giannaris C, Rubio A. Advanced Materials 2000;12:750.
[30] Shaffer M, Kinloch IA. Composites Science and Technology 2004;64: 2281.
[31] Hutchison JL, Kiselev NA, Krinichnaya EP, Krestinin AV, Loufty RO, Morawsky AP, et al. Carbon 2001;39:761.
[32] Saito Y, Nakahira T, Uemura S. Journal of Physical Chemistry B 2003; 107:931.
[33] Zhang Y, Iijima S. Applied Physics Letters 1999;75:3087.
[34] Scott CD, Arepalli S, Nikolaev P, Smalley RE. Applied Physics A 2001; 72:573.
[35] Arepalli S. Journal of Nanoscience and Nanotechnology 2004;4:317.
[36] Jiang W, Molian P, Ferkel H. Journal of Manufacturing Science and Engineering 2005;127:703.
[37] Hiraoka T, Kawakubo T, Kimura J, Taniguchi R, Okamuto A, Okazaki T, et al. Chemical Physics Letters 2003;382:679.
[38] Darabont Al, Nemes-Incze P, Kertész K, Tapaszó L, Koós AA, Osváth Z, et al. Journal of Optoelectronics and Advanced Materials 2005;7:631.
[39] Aghababazadeh R, Mirhabibi AR, Ghanbari H, Chizari K, Brydson RM, Brown AP. Journal of Physics: Conference Series 2006;26:135.
[40] Endo M, Hayashi T, Kim YA, Muramatsu H. Japanese Journal of Applied Physics 2006;45:4883.
[41] Sugai T, Yoshida H, Shimada T, Okazaki T, Shinohara H, Bandow S. Nano Letters 2003;3:769.
[42] Sugai T, Okazaki T, Yoshida H, Shinohara H. New Journal of Physics 2004;6:21.
[43] Thostenson ET, Ren Z, Chou T-W. Composites Science and Technology 2001;61:1899.
[44] Moniruzzaman M, Winey KI. Macromolecules 2006;39:5194.
[45] Pham JQ, Mitchell CA, Bahr JL, Tour JM, Krishanamoorti R, Green PF. Journal of Polymer Science, Part B: Polymer Physics 2003; 41:3339.
[46] Xie H, Liu B, Yuan Z, Shen J, Cheng R. Journal of Polymer Science, Part B: Polymer Physics 2004;42:3701.
[47] Gojny FH, Wichmann MHG, Köke U, Fiedler B, Schulte K. Composites Science and Technology 2004;64:2363.
[48] Du F, Fischer JE, Winey KI. Journal of Polymer Science, Part B: Polymer Physics 2003;41:3333.
[49] Gorga RE, Cohen RE. Journal of Polymer Science, Part B: Polymer Physics 2004;42:2690.
[50] Dondero WE, Gorga RE. Journal of Polymer Science, Part B: Polymer Physics 2006;44:864.
[51] Kim JY, Kim SH. Journal of Polymer Science, Part B: Polymer Physics 2006;44:1062.
[52] Yu Y, Ouyang C, Gao Y, Si Z, Chen W, Wang Z, et al. Journal of Polymer Science, Part A: Polymer Chemistry 2005;43:6105.
[53] Ham HT, Choi YS, Chee MG, Chung IJ. Journal of Polymer Science, Part A: Polymer Chemistry 2006;44:573.
[54] Kwon J, Kim H. Journal of Polymer Science, Part A: Polymer Chemistry 2005;43:3973.
[55] Gojny F, Schulte K. Composites Science and Technology 2004;64:2303.
[56] Ramanathan T, Liu H, Brinson LC. Journal of Polymer Science, Part B: Polymer Physics 2005;43:2269.
[57] Wu H-L, Yang Y-T, Ma C-CM, Kuan H-C. Journal of Polymer Science, Part A: Polymer Chemistry 2005;43:6084.
[58] Gong X, Liu J, Baskaran S, Voise RD, Young JS. Chemistry of Materials 2000;12:1049.
[59] Kónya Z, Vesselenyi I, Niesz K, Kukovecz A, Demortier A, Fonseca A, et al. Chemical Physics Letters 2002;360:429.
[60] Bahr JL, Yang J, Kosynkin DV, Bronikowski M, Smalley RE, Tour JM. Journal of the American Chemical Society 2001;123:6536.
[61] Zhang N, Xie J, Guers M, Varadan VK. Smart Materials and Structures 2004;13(N1).
[62] Zhu J, Kim JD, Peng H, Margrave JL, Khabashesku VN, Barrera EV. Nano Letters 2003;3:1107.
[63] Zhu J, Peng H, Rodriguez-Macias F, Margrave JL, Khabashesku VN, Imam AM, et al. Advanced Functional Materials 2004;14:643.
[64] Wang J, Fang Z, Gu A. Polymer Engineering and Science 2006;46:635.
[65] Pompeo F, Resasco DE. Nano Letters 2002;2:369.
[66] Odegard GM, Frankland SJV, Gates TS. American Institute of Aeronautics and Astronautics Journal 2005;43:1828.
[67] Kooi SE, Schlecht U, Burghard M, Kern K. Angewandte Chemie International Edition 2002;41:1353.
[68] Balasubramanian K, Friedrich M, Jiang C, Fan Y, Mews A, Burghard M, et al. Advanced Materials 2003;15:1515.
[69] Bahun GJ, Wang C, Andronov A. Journal of Polymer Science, Part A: Polymer Chemistry 2006;44:1941.
[70] Narain R, Housni A, Lane L. Journal of Polymer Science, Part A: Polymer Chemistry 2006;44:6558.
[71] Ha JU, Kim M, Lee J, Choe S, Cheong IW, Shim SE. Journal of Polymer Science, Part A: Polymer Chemistry 2006;44:6394.
[72] Huang W, Lin Y, Taylor S, Gaillard J, Rao AM, Sun Y-P. Nano Letters 2002;2:231.
[73] Lu KL, Lago RM, Chen YK, Green MLH, Harris PJF, Tsang SC. Carbon 1996;34:814.
[74] Clément F, Lapra A, Bokobza L, Monnerie L, Ménez P. Polymer 2001; 42:6259.
[75] Dannenberg EM. Rubber Chemistry and Technology 1975;48:410.
[76] Kraus G. Interactions between elastomers and reinforcing fillers. In: Kraus G, editor. Reinforcement of elastomers. New York: Wiley; 1965. p. 125–52.
[77] Kraus G. Reinforcement of elastomers by carbon black. Advances in Polymer Science 1971;8:155.
[78] Wagner MP. Rubber Chemistry and Technology 1976;49:703.
[79] Voet A. Journal of Polymer Science: Macromolecular Reviews 1980;15: 327.
[80] Edwards DC. Journal of Materials Science 1990;25:4175.
[81] Ahmed S, Jones FR. Journal of Materials Science 1990;25:4933.
[82] Payne AR. In: Kraus G, editor. Reinforcement of elastomers. New York: Interscience Publishers; 1965. p. 69.
[83] Wang M-J. Rubber Chemistry and Technology 1998;71:520.
[84] Mullins L. Rubber Chemistry and Technology 1969;42:339.
[85] Bueche F. Journal of Applied Polymer Science 1960;4:107.
[86] Clément F, Bokobza L, Monnerie L. Rubber Chemistry and Technology 2001;74:847.
[87] Grosch KA, Harwood JAC, Payne AR. Rubber Chemistry and Technology 1968;41:1157.
[88] Harwood JAC, Payne AR. Journal of Applied Polymer Science 1968; 12:889.
[89] Salvetat J-P, Briggs GAD, Bonard J-M, Bacsa RR, Kulik A, Stöckli T, et al. Physical Review Letters 1999;82:944.
[90] Poncharal P, Wang ZL, Ugarte D, de Heer WA. Science 1999;283: 1513.
[91] Yu M-F, Lourie O, Dyer MJ, Moloni K, Kelly TF, Ruoff RS. Science 2000;287:637.
[92] Allaoui A, Bai S, Cheng HM, Bai JB. Composites Science and Technology 1993;62:2002.
[93] Tai N-H, Yeh M-K, Liu J-H. Carbon 2004;42:2774.
[94] Yeh M-K, Tai N-H, Liu J-H. Carbon 2006;44:1.
[95] Qian D, Dickey EC, Andrews R, Rantell T. Applied Physics Letters 2000;76:2868.
[96] McNally T, Pötschke P, Halley P, Murphy M, Martin D, Bell SEJ, et al. Polymer 2005;46:8222.
[97] Atieh MA, Girun N, Ahmadun F-R, Guan CT, Mahdi A-S, Baik DR, et al. Journal of Nanotechnology 2005;1:1 [Online].
[98] Miltner HE, Peeterbroeck S, Viville P, Dubois P, Van Mele B. Journal of Polymer Science, Part B: Polymer Physics 2007;45:1291.
[99] Odegard GM, Gates YS, Wise KE, Park C, Siochi EJ. Composites Science and Technology 2003;63:1671.
[100] Fornes TD, Paul DR. Polymer 2003;44:4993.
[101] Ramsteiner F, Theysohn R. Composites 1984;15:121.
[102] Guth E. Journal of Applied Physics 1945;16:20.
[103] Halpin JC. Journal of Composite Materials 1969;3:732.

[104] Lapra A, Clément F, Bokobza L, Monnerie L. Rubber Chemistry and Technology 2003;76:60.
[105] Medalia AI. Rubber Chemistry and Technology 1978;51:437.
[106] Bokobza L, Gaulliard V, Ladouce L. Kautschuk Gummi Kunststoffe 2001;54:177.
[107] Fragiadakis D, Pissis P, Bokobza L. Polymer 2005;46:6001.
[108] Kraus G, Gruver JT. Journal of Polymer Science 1970;A2(8):571.
[109] Pötschke P, Fornes TD, Paul DR. Polymer 2002;43:3247.
[110] Ding W, Eitan A, Fisher FT, Chen X, Dikin DA, Andrews R, et al. Nano Letters 2003;3:1593.
[111] Clément F, Bokobza L, Monnerie L. Rubber Chemistry and Technology 2005;78:211;
Rubber Chemistry and Technology 2005;78:232.
[112] Bokobza L, Kolodziej M. Polymer International 2006;55:1090.
[113] Cooper CA, Young RJ, Halsall M. Composites: Part A 2001;32:401.
[114] Flandin L, Chang A, Nazarenko S, Hiltner A, Baer E. Journal of Applied Polymer Science 2000;76:894.
[115] Thongruang W, Balik CM, Spontac RJ. Journal of Polymer Science, Part B: Polymer Physics 2002;40:1013.
[116] Payne AR. Journal of Applied Polymer Science 1965;9:1073.
[117] Payne AR, Whittaker RE. Rubber Chemistry and Technology 1971;44: 440.
[118] Donnet J-B, Voet A, editors. Carbon. New York and Basel: Marcel Dekker, Inc.; 1976.
[119] Sau KP, Chaki TK, Khastgir D. Journal of Applied Polymer Science 1999;71:887.
[120] Das NC, Chaki TK, Khastgir D. Polymer International 2002;51:156.
[121] Yamaguchi K, Busfield JJ, Thomas AG. Journal of Polymer Science, Part B: Polymer Physics 2003;41:2079.

Liliane Bokobza graduated in Physics and Chemistry from the University of Paris. She earned her Ph.D. at the University of Paris in Vibrational Spectroscopy. She is currently Professor of Spectroscopy at Ecole Supérieure de Physique et de Chimie Industrielles de la Ville de Paris (ESPCI). She was promoted Chevalier of the Legion of Honour in 1999, got the George Stafford Whitby Award from the Rubber Division of the American Chemical Society in 2002 and the Jean Langlois Award for her research activities in Paris (november, 2002).

Liliane Bokobza has been involved in many areas of research in polymer science including investigation of local dynamics of macromolecular chains in bulk elastomeric systems by the excimer fluorescence technique, analysis of molecular orientation in elastomeric networks by infrared dichroism, reinforcement of elastomers by mineral fillers, and new developments in vibrational spectroscopy. Liliane Bokobza's work has been in over 120 publications, several book chapters and she is frequently invited to give lectures in her areas of expertise.